sciendo

DOI 10.2478/ama-2023-0043

acta mechanica et automatica, vol.17 no.3 (2023)

STABILITY INVESTIGATION OF THE PCM NANOCOMPOSITES

Janusz T. CIEŚLIŃSKI*, Paulina BOROŃ*, Maciej FABRYKIEWICZ*

*Faculty of Mechanical Engineering and Ship Technology, Institute of Energy, Gdańsk University of Technology, ul. Narutowicza 11/12, 80-233 Gdańsk, Poland

jcieslin@pg.edu.pl, s166585@student.pg.edu.pl, mac.fabrykiewicz@gmail.com

received 21 September 2022, revised 13 March 2023, accepted 19 March 2023

Abstract: Ensuring the stability is a key issue to be solved for the technical application of nanocomposites. In this work, fatty acid P1801 served as base phase change material (PCM)P1801, and its main ingredients are palmitic acid (58%) and stearic acid (38%). Titania (TiO2) and alumina (Al2O3) with mass concentrations of 1% and 5% were selected as nanoparticles, while polyvinylpyrrolidone (PVP) or oleic acid (OA) with mass concentrations of 5% were tested as surfactants. On the basis of the measured temperature distributions in the sample, which is subject to melting and solidification processes, it was determined which of the tested nanocomposites are stable and which are not. In addition, a thermal test was proposed to assess the stability of the produced nanoPCM, which consists in measuring the temperature distribution versus time according to a precisely given procedure.

Key words: stability, nanoPCM, experiment, surfactant, alumina, titania, concentration

1. INTRODUCTION

The main obstacle to the widespread use of materials containing nanoparticles is their stability. This applies to both nanofluids and nanocomposites (nanoPCMs) [1–8]. While in the case of nanofluids there are reliable methods of determining their stability [9–11], in the case of nanocomposites these methods are still being developed. Wu et al. [12] studied the stability of paraffin-Cu-surfactant nanocomposites through heat capacity measurement by the use of differential scanning calorimetric (DSC). Although the heat transfer rate of nanoPCM was improved, the latent heats and the melting and freezing temperatures change very little after 100 thermal cycles. Choi et al. [13] tested the stability of stearic acid-carbon additives (multi-walled carbon nanotubes [MWCNT], CNT and graphene) nanocomposites by direct observation of examined nanoPCMs in the liquid state in a thermal chamber at a constant temperature. Jin et al. [14] proposed a thermal cycling test to evaluate the influence of the fabrication method of paraffin wax-expanded graphite nanocomposites on their thermal stability. A single test consisted of a melting and solidification process. Based on the time course of temperature, Jin et al. [14] found that both nanoPCMs produced in vacuum and those produced at atmospheric pressure were thermally stable. Zhichao et al. [15], basing their study on the Fourier transform infrared spectroscopy (FT-IR) spectrum, established that the optical micrographs of erythritol-TiO_2 nanocomposite with nanoparticles higher than 0.2%vol were more blurry than that for pure erythritol. Moreover, the solidification microstructure was changed. Nourani et al. [16] examined the stability of thermal properties (melting temperature and phase change enthalpy) of parafin-Al_2O_3 nanocomposites and stated that the DSC analysis after many melting/solidification cycles does not provide information on the stability of the nanocomposite. Measurement of the melting point does not provide information about the stability of the nanoPCM, as it depends on chemical decay. In turn, the latent heat of fusion is an intensive property. Liu and Yang [17] used scanning electron microscopy (SEM) to study the microstructure and optical microscopy to examine the crystallography features of eutectic hydrate salt-α-Al_2O_3 nanocomposite. Singh et al. [18], using field emission scanning electron microscopy (FESEM), determined that the distribution of CuO nanoparticles in the Myo-inositol based nanocomposite was more uniform than that observed in the case of Al_2O_3 nanoparticles. Zhang et al. [19] studied the surface morphology and the chemical structure of stearic acid-expanded graphite nanocomposite by use of an SEM and an FT-IR spectrometer, respectively. Nourani et al. [20] evaluated the stability of the paraffin-γ-Al_2O_3-surfactant nanocomposite by the use of spectrophotometry and measurement of Al^{3+} concentration. Prabhu and ValanArasu [21] examined the stability of the paraffin wax-TiO_2–Ag nanocomposites by visual analysis of the sedimentation photographs 12 h after nanoPCM production. Ibrahim et al. [22], based on the fact that the addition of nanoparticles to paraffin causes a change in the absorbance and transmittance of the mixture, proposed an optical method for determining the stability of the paraffin-TiO_2/MgO nanocomposite. It was observed that the absorbance of the tested nanocomposites depends on the type and concentration of added nanoparticles. In turn, the transmittance for nanocomposites with a mass concentration of 1% changes significantly for short wavelengths and is stable for long wavelengths. To examine the distribution and dispersion of nanoparticles on the surface of the samples, Ibrahim et al. [22] used FESEM and energy dispersive spectroscopy (EDS). Zhang et al. [23] analysed the stability of nanophase change emulsions both by direct observation and particle size distribution and particle dispersion index (PDI) measurements. Venkateshwar et al. [24] analysed the potential techniques to quantify the concentration of nanoparticles after each melting–solidification cycle on nanoPCM. Limitations of the application of the thermal conductivity measurement, viscosity measurement, heat capacity measurement and microscopy for quanti-

DOI 10.2478/ama-2023-0043

fication of the nanoparticle concentration have been discussed. Instead, Venkateshwar et al. [24] have proposed a novel image analysis technique to measure the concentration and non-uniformity in the dispersion of nanoparticles in a vial of 4 cm height placed in the thermal bath. The method consists in making digital images of the sample, which are then converted to the red-green-blue (RGB) scale. Then, the RGB scale is converted to a hue-saturation-lightness (HSL) scale. A correlation between an individual component of the RGB and HSL scales and nanoparticles concentration has to be developed. The lightness (L) was observed to closely follow the change in the nanoparticle concentration. It was established that the rate of sedimentation depends on the density difference in the solid and liquid states of phase change material (PCM). Moreover, the effect of particle size dominates over nanoparticles density in the sedimentation process. Recently, the role of particle/molecules polarity has been highlighted in studies of the stability of nanocomposites [25–28]. Saydam and Duan [25] conducted a comprehensive study on the stability of the paraffin-based nanocomposites by use of visualisation and thermal conductivity measurement. Three different types of nanoparticles were tested, i.e. MWCNT, graphene nanoplatelets (GNP) and Al_2O_3. Significant coagulation and deposition of nanoparticles were found after a few thermal cycles regardless of the nanoparticle type, concentration or dispersion method (sonication, stirring). Different boundary conditions in heating were also examined for their effects. All tested nanocomposites showed an insignificant increase in thermal conductivity due to the agglomeration and sedimentation of nanoparticles. According to Saydam and Duan [25], the fundamental reason is related to the chemical nature of the PCM and nanoparticles: the paraffin wax has nonpolar molecules while all the tested nanoparticles have polar molecules. Saroha et al. [28] tested the stability of paraffin-TiO_2 and sorbitol-TiO_2 nanoPCMs. According to the authors' concept, the paraffin-TiO_2 nanoPCM is thermally unstable, because n-alkane chains that create paraffin wax are nonpolar and TiO_2 nanoparticles are polar. Contrary to paraffin wax, sorbitol molecules are polar; therefore, sorbitol-TiO_2 nanoPCM is thermally stable.

According to the literature review, the methods for determining the stability of nanoPCM can be divided into several groups. The first method, the simplest, is the direct observation of the produced nanoPCMs over time. The second group includes the use of SEM to determine the microstructure of nanocomposites. The third group of methods is based on ascertainment of the optical properties of produced nanoPCM using spectrophotometry. The next group of methods is based on the measurements of thermophysical properties of the produced nanoPCM, with the use of DSC. Measurements of nanoparticle distribution and concentration are also used to determine the stability of nanoPCMs. Finally, the measurements of the rate of heating and cooling of nanoPCM during the melting and solidification process should be distinguished.

In the present study, the stability of a nanoPCM, composed of base PCM, nanoparticles and surfactant, was investigated. Fatty acid P1801 served as base PCM, and its main ingredients are palmitic acid (58%) and stearic acid (38%). As nanoparticles, TiO_2 and Al_2O_3 with mass concentrations of 1% and 5% were used. Polyvinylpyrrolidone (PVP) or oleic acid (OA) with mass concentrations of 5% were selected as surfactants. The nanoPCMs were fabricated by the use of a two-step method in the liquid phase.

The paper presents the original results of stability studies of a series of fatty acid-based nanocomposites. Moreover, the effect of nanoparticles on the rate of heat transfer during the process of heating and cooling nanoPCM was assessed. Finally, a simplified nanoPCM stability test was proposed, consisting in measuring the temperature in the sample with a single resistance thermometer placed along the axis of the sample in the middle of its height. The method used is an extension of the thermal cycling test proposed by Jin et al. [14]. However, while in the method of Jin et al. [14] the solidification process took place immediately after the melting process, in the present test, between the melting and solidification stages, there is a period of 12 h of keeping the nanoPCM at ambient temperature. It is believed that this is a more realistic representation of the operating mode of the thermal energy storage, which may affect the stability of the nanoPCM. In addition, the method of measuring the temperature of the nanoPCM sample was precisely defined, which was not specified in the study of Jin et al. [14].

2. MATERIALS AND METHODS

2.1. Materials

An organic commercial material fatty acid, P1801, supplied by Konimpex Chemicals (Konimpex Chemicals, Konin, Poland), was used as a base material. The detailed chemical composition of the tested material was determined on the basis of chromatographic tests using the GC-MS-QP2010 PLUS (Shimadzu Corp., Kyoto, Japan) . The results of the analysis are presented in Fig. 1.

The range of phase transition temperatures, heat of phase transition and specific heat of the tested base material were estimated by the DSC method using DSC 404 F1 Pegasus instrument (Netzsch Gmbh, Selb, Germany). The results of the analysis are presented in Fig. 2.

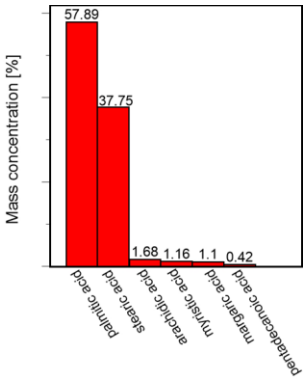

Fig. 1. Results of the chromatographic analysis of P1801

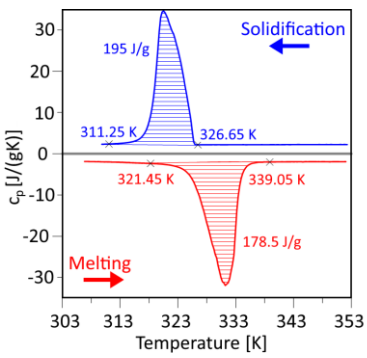

Fig. 2. Results of the DSC analysis of P1801. DSC, differential scanning calorimetric

The tested nanoparticles were titania (TiO_2) and alumina (Al_2O_3), supplied by Sigma Aldrich Ltd. (Merck, KGaA, Damstadt, Germany). Mass concentrations of particles in the composites were 1% and 5%. SEM images of the used nanoparticles are shown in Fig. 3.

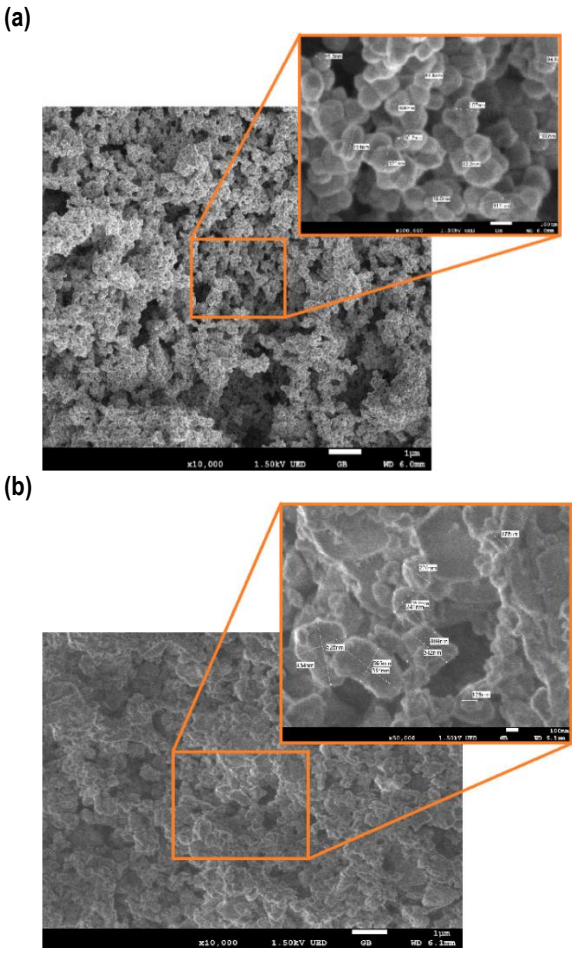

Fig. 3. SEM images of the nanoparticles; (a) TiO2, (b) Al2O3. SEM, scanning electron microscopy

Tab. 1. List of the tested PCMs

Sample	Melting	Solidification	Surfactant (wt [%])	Nanoparticles (wt [%])
nanoPCM1	nM1	nS1	OA (5%)	Al_2O_3 (1%)
nanoPCM2	nM2	nS2		Al_2O_3 (5%)
nanoPCM3	nM3	nS3		TiO_2 (1%)
nanoPCM4	nM4	nS4		TiO_2 (5%)
nanoPCM5	nM5	nS5	PVP (5%)	Al_2O_3 (1%)
nanoPCM6	nM6	nS6		Al_2O_3 (5%)
nanoPCM7	nM7	nS7		TiO_2 (1%)
nanoPCM8	nM8	nS8		TiO_2 (5%)
BPCM	BM	BS	-	-

BPCM, base phase change material; OA, oleic acid; PCMs, phase change materials; PVP, polyvinylpyrrolidone

The following surfactants were used to prepare nanocomposites: OA supplied by Warchem Ltd. (Warchem Ltd., Warsaw, Poland) and PVP supplied by Keten Ltd.(Keten Ltd., Wrocław, Poland).

A two-step method was used to prepare the tested nanoPCM. The process of producing nanoPCM started with melting the base phase change material (BPCM) in the container in a water bath at a temperature of 343 K. The melted BPCM was poured into measuring tanks in the amount of 80 g. The selected surfactant was added to the melted BPCM at a mass concentration of 5% and premixed. Then, nanoparticles in an amount corresponding to mass concentrations of 1% and 5% were added to the mixture prepared and mixed again. The containers with the prepared samples were placed in an ultrasonic cleaner for a period of 45 min. The list of nanoPCMs tested is presented in Tab. 1.

2.2. Apparatus and instrumentation

The setup consisted of a thermostat EBR^c produced by Prüfgeräte-Werk Medingen (MLW, Medingen, Germany) and a computer-aided data acquisition system. The scheme of the experimental setup is shown in Fig. 4. A set of four containers with nanoPCM were simultaneously immersed in a water bath. The containers were made of glass, ensuring direct observation of the tested samples. Each container was equipped with a resistance thermometer placed halfway up the container axis.

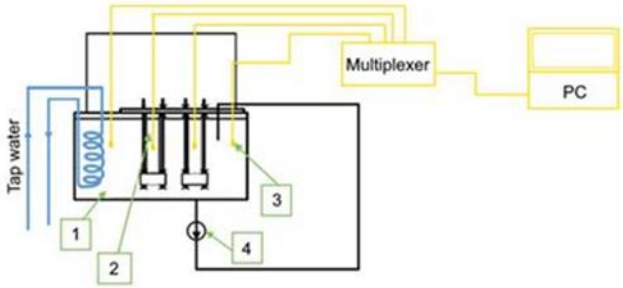

Fig. 4. Scheme of the experimental setup scheme: 1 – thermostat, 2 – set of containers with PCM, 3 – resistance thermometer, 4 – circular pump. PCM, phase change material

2.3. Methods

A single cycle included three measurement stages (Fig. 5). The first stage was started by placing the prepared molten sample at 343 K in a water bath of a thermostat at 293 K. During the solidification of the sample, the temperature was recorded using a resistance thermometer Pt100 (Termoaparatura Wrocław, Wrocław, Poland). The temperature values were recorded every 10 s. The measurement was performed until the temperature reading from the resistance thermometer did not deviate from 293 K by ± 0.5 K for 5 min. When the sample reached the expected temperature, it was removed from the water bath and left at the ambient parameters for about 20 min. After this time, the sample was placed again in the water bath at 343 K. The temperature measurement was carried out until the sample melted, i.e. it reached the temperature of 343 ± 0.5 K, and then the sample remained at the ambient temperature for 12 h. The second stage of the cycle started with the process of melting the sample in a water bath at a temperature of 343 K. The process was carried out until the sample reached the water bath temperature (± 0.5 K). Then the sample was placed in the water bath for about 20 min. After this time, the sample was placed back in the water bath at 293 K. After solidification, the sample was kept at ambient temperature for 12 h. The

DOI 10.2478/ama-2023-0043

third step was essentially a repetition of the second step, except for the 12-h phase involving keeping the sample at ambient temperature.

A simplified nanoPCM stability test was proposed, consisting in measuring the temperature in the sample according to the three-stage procedure involving three melting and three solidification processes. If the time of reaching the melting temperature T_t'' or solidification temperature T_k' of the nanoPCM after the third melting or solidification processes does not differ by more than 5% compared to the first melting or solidification processes, it can be assumed that the nanoPCM is stable.

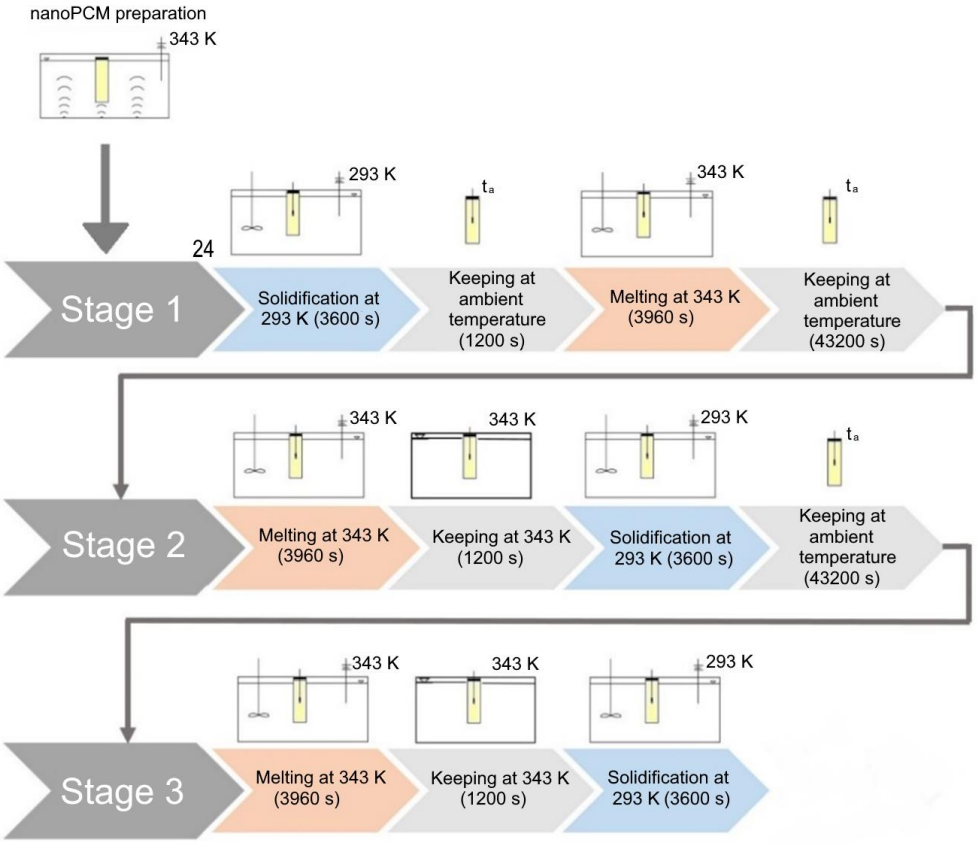

Fig. 5. Flow chart of the research cycle

3. RESULTS AND DISCUSSION

In order to check the measurement procedure and the reproducibility of the results, a full test cycle was performed for the BPCM according to the measurement procedure described in Section 2.3. Figures 6a and 6b show the temperature courses during the three melting processes (Run1, Run2 and Run3) and solidification processes (Run1, Run2 and Run3) of the tested BPCM, respectively. The black lines in Fig. 6 (BM_{AV} and BS_{AV}) represent the average temperature calculated as an arithmetic mean of three runs for the melting and solidification processes, respectively. As shown in Fig. 6a, the temperature courses during the solidification processes, which took place every 15 h, practically overlap. The time after which the T_k' temperature was reached for the second solidification process (Run2) was about 4.7% longer in comparison with those for the first (Run1) and third (Run3) solidification processes. As can be seen in Fig. 6b, the time to reach the melting temperature T_t'' was the same in all three melting processes (Run1, Run2 and Run3). The average times, calculated in each case as an arithmetic mean for the three processes, to reach the temperatures T_t'' and T_k' for BPCM were 2,190 s and 2,528 s, respectively.

In order to determine the stability of the tested nanoPCMs, the temperature courses were analysed for the three solidification and melting processes carried out according to the proposed procedure (Section 2.3). The obtained temperature courses are presented in Fig. 7. It is noticeable that nanoPCM1, nanoPCM2, nanoPCM5 and nanoPCM6 present the convergence of the temperature course of their cycles in the solidification process. For the melting process, this convergence is visible for nanoPCM1, nanoPCM5 and nanoPCM7.

As can be seen in Fig. 7a, the time to reach the melting temperature T_t'' for nanoPCM1 was almost the same for the first and second melting processes (Run1 and Run2), while it was about 5% longer for the third solidification process (Run3) compared to the first process (Run1). In the case of the solidification process, the time of reaching T_k' for nanoPCM1 was almost the same in all three solidification processes (Run1, Run2 and Run3). So, it can be concluded that nanoPCM1 is relatively stable. It is worth noting that in the case of BPCM, the times to achieve T_k' and T_t'' were

shorter by about 10% and 5% compared to nanoPCM1, which indicates heat transfer deterioration when using nanoPCM1.

Fig. 7b shows that the time of reaching the melting temperature T_t'' for nanoPCM2 increases with the number of repetitions and is longer for Run2 and Run3 compared to Run1 by about 4% and 13%, respectively. The temperature courses for two solidification processes (Run1 and Run2) almost overlap. However, for the third process (Run3), the time to reach the temperature T_k' was about 4% longer compared to Run1. Hence, due to the systematic increase in melting and solidification times in subsequent runs, nanoPCM2 cannot be considered stable. As for nanoPCM1, it was observed that adding Al_2O_3 with a mass concentration of 5% to BPCM deteriorated heat transfer. In the case of nanoPCM2, this applies to both the melting and solidification processes, for which the time to reach T_t'' and T_k' was about 10% longer than for BPCM.

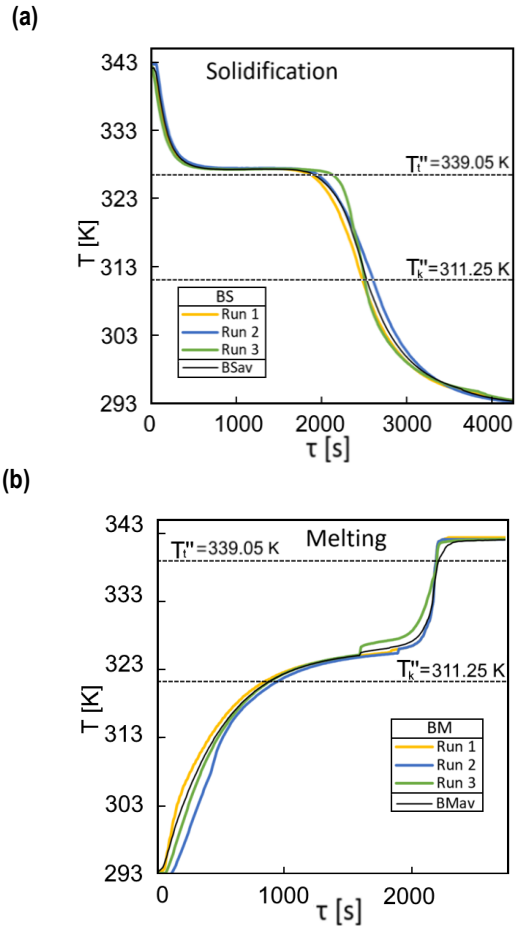

Fig. 6. Temperature courses for BPCM (a) solidification; (b) melting. BPCM, base phase change material

Fig. 7c shows the temperature courses for nanoPCM3. In the case of the melting process, the time to reach T_t'' for subsequent runs slightly increases and is, respectively, about 2% and 3% longer for Run2 and Run3, compared to Run1. For the solidification process, the time to reach the temperature T_k' increases by about 5% for Run2 and about 15% for Run3 compared to Run1. Therefore, nanoPCM3 cannot be treated as stable. However, it is worth noting that the addition of TiO_2 nanoparticles with a mass concentration of 1% improved heat transfer, especially for the melting process for which the time to reach T_t'' for BPCM was about 15% shorter than that observed for nanoPCM3.

Fig. 7d shows the temperature courses for nanoPCM4. It is seen that the time to reach the melting temperature T_t'' increases substantially from run to run, and is about 12% and 40% longer for Run2 and Run3, respectively, compared to Run1. A similar trend is observed for the solidification process, where the time to reach T_k' is about 18% and 25% for Run2 and Run3, respectively, compared to Run1. Therefore, the nanoPCM4 should be treated as highly unstable. The intensification of heat transfer in the melting process is noteworthy, which admittedly decreases with each subsequent run, but the time to reach the melting temperature T_t'' during Run3 is about 15% longer than for BPCM.

As seen in Fig. 7e, the time to reach the melting temperature T_t'' for nanoPCM5 increases for each subsequent run, and finally for Run3 is about 40% longer than for BPCM. However, the addition of Al_2O_3 nanoparticles with a mass concentration of 1% with PVP as a surfactant has no effect on the solidification process. The temperature courses for all three runs (Run1, Run2 and Run3) are almost identical. Therefore, the nanoPCM4 should be treated as highly unstable. Moreover, the addition of Al_2O_3 nanoparticles with a mass concentration of 1% with PVP as a surfactant deteriorates heat transfer. The times to reach T_t'' and T_k' for nanoPCM5 are longer than for BPCM.

Fig. 7f shows the temperature courses for nanoPCM6. For the melting process, the times to reach temperature T_t'' for Run1 and Run2 are almost identical. However, the time to reach the melting temperature for Run3 is longer by about 15% compared to that observed for Run1. For the solidification process, the times to reach the temperature T_k' were almost the same for all the three runs. Nevertheless, nanoPCM6 cannot be considered stable. The addition of Al_2O_3 nanoparticles with a mass concentration of 5% with PVP as a surfactant slightly deteriorates heat transfer. The time extension to reach the temperatures T_t'' and T_k' for the third runs compared to BPCM was about 35% for the melting process and 8% for the solidification process.

Fig. 7g shows the temperature courses for nanoPCM7. For the melting process, after Run1 a kind of stabilisation is observed – the temperature courses for Run2 and Run3 overlap with each other. For the solidification process, the temperature courses for all three runs are almost identical. On this basis, nanoPCM7 can be considered stable. However, the addition of TiO_2 nanoparticles with a mass concentration of 1% and PVP as a surfactant slightly deteriorates heat transfer during the melting process. The time to reach temperature T_t'' for Run3 is about 13% longer compared to BPCM. The time to reach solidification temperature T_k' for nanoPCM7 is identical as for BPCM.

Fig. 7h shows the temperature courses for nanoPCM8. The time to reach the melting temperature T_t'' increases for each subsequent run and finally for Run3 is about 19% longer than for Run1. For the solidification process, the times to reach temperature T_t'' for Run1 and Run2 are nearly the same, while for Run3 the time extension was about 7% compared to Run1. On this basis, it was assessed that nanoPCM8 is not stable. The divergent impact of TiO_2 nanoparticles with a mass concentration of 5% and PVP as a surfactant on heat transfer can be observed. For Run1, during the melting process, a heat transfer improvement is observed – the time to reach temperature T_t'' is shorter by about 6% compared to that observed for BPCM. For Run2 and Run3, deterioration of heat transfer is noted – the time to reach temperature T_t'' for Run3 is longer by about 12% compared to that observed for BPCM. For the solidification process, a slight improvement of heat transfer was

DOI 10.2478/ama-2023-0043

observed for Run1 and Run2, and a slight deterioration of heat transfer was observed for Run3 compared to BPCM.

During the melting process, free convection dominates, which favours the possible sedimentation of nanoparticles. The melting process proceeds from the glass wall of the vessel with the nanoPCM sample towards the core in which the resistance thermometer is located. The front of the molten nanoPCM moves in an axisymmetric manner because the vessel with the nanoPCM sample is positioned vertically and is immersed in a large volume of liquid at a constant temperature (controlled by a thermostat). Initially, the layer of liquid nanoPCM is very thin and practically immobile.

As the layer thickness increases, the molten nanoPCM rises upwards along the vessel wall. The upward movement also results from the fact that the bottom of the cell is heated and the top of the sample is not heated. Fulfilling the mass continuity balance requires that the liquid nanoPCM that has reached the free surface begins to flow down, melting the solid nanoPCM around the resistance thermometer.

The solidification process starts from the vessel wall and the front of the solidified nanoPCM moves in an axisymmetric manner towards the core, which is in the liquid state. The heat transfer process is dominated by heat conduction, which means that the time of nanoPCM solidification is much longer compared to that involved in the melting process. Due to the axisymmetric nature of the heat transfer, there is no need to measure the angular temperature distribution, and accordingly it was decided to place the thermal resistance thermometer in the axis of the vessel.

The assessment of the stability of nanoPCM consists in maintaining the same temperature course after several cycles including the process of melting and solidification. It is assumed that the addition of nanoparticles improves heat conduction, and thus, above all, a shortening of the solidification time. The melting and solidification time of nanoPCM should be shorter than that of BPCM. The shift of the temperature distribution curves for nanoPCM towards the temperature distributions obtained for BPCM indicates the sedimentation of nanoparticles, and thus the lack of stability.

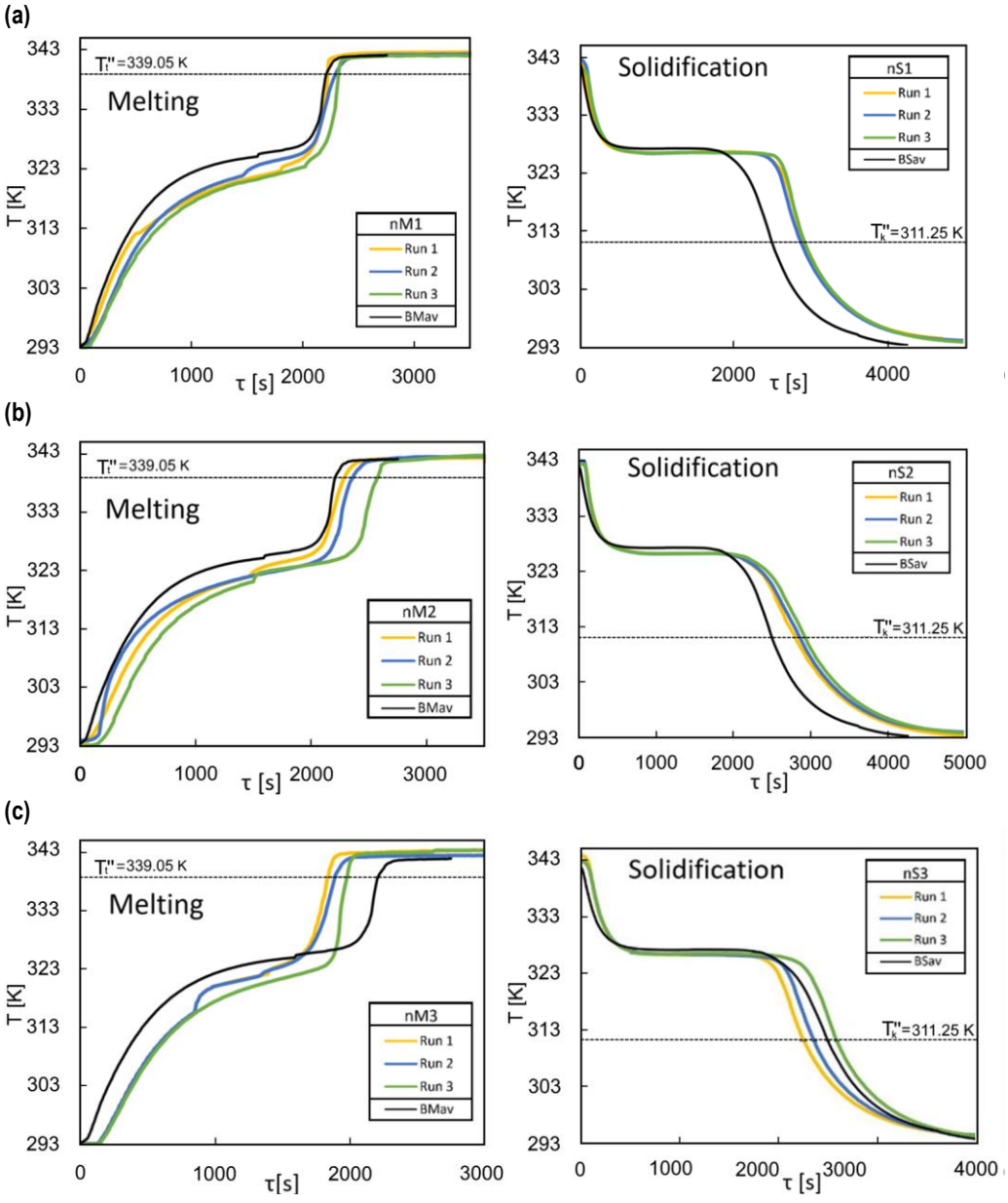

(d)

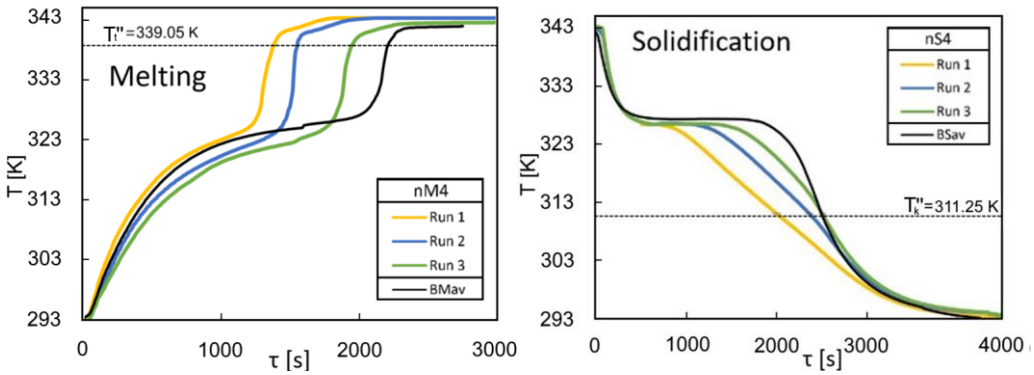

(e)

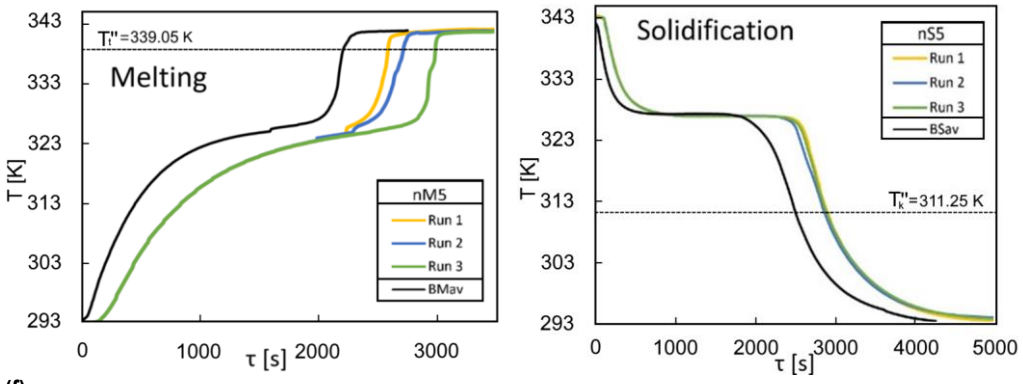

(f)

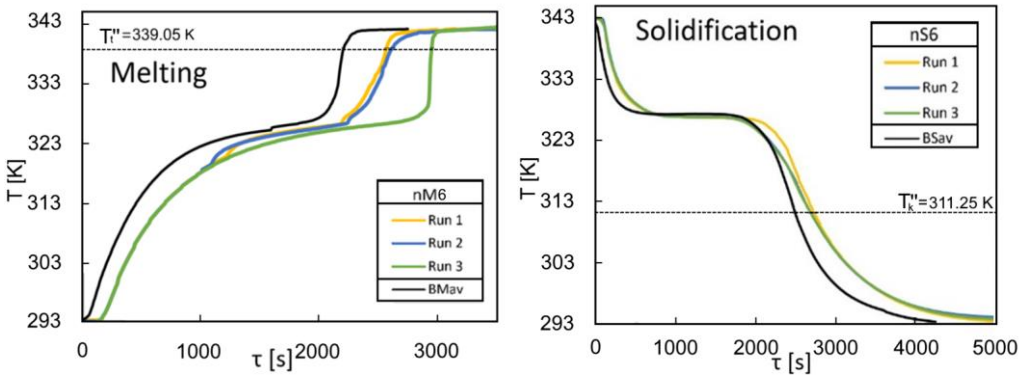

(g)

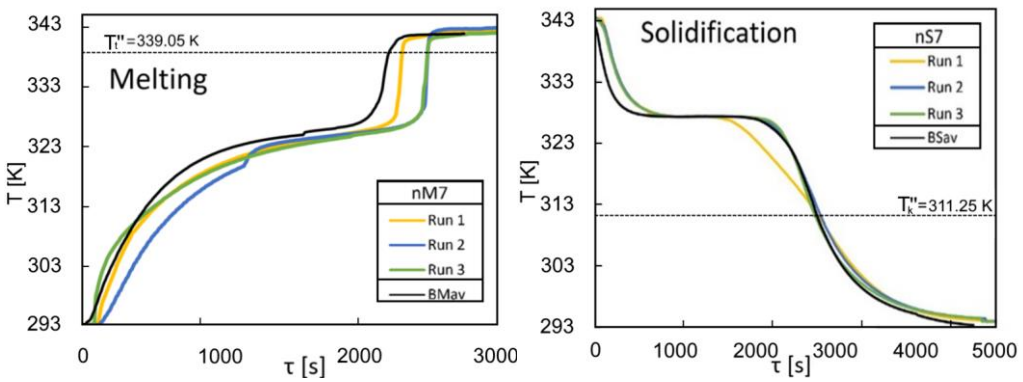

DOI 10.2478/ama-2023-0043

(h)

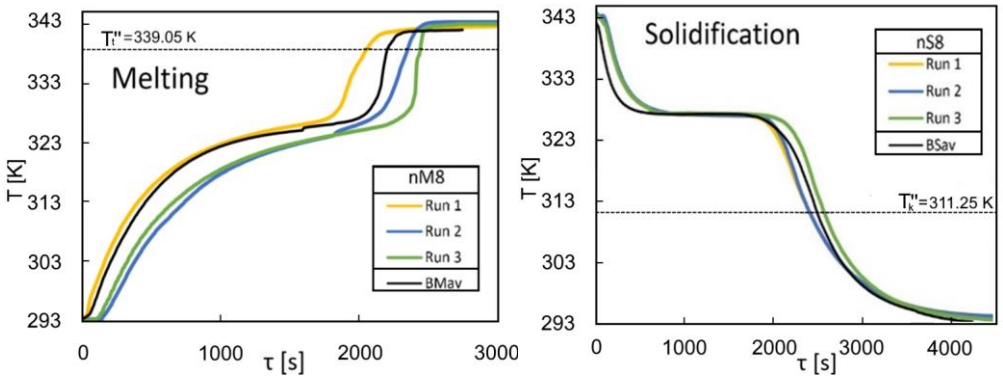

Fig. 7. Temperature courses for the melting and solidification processes of nanoPCM; (a) nanoPCM1; (b) nanoPCM2;(c) nanoPCM3; (d) nanoPCM4; (e) nanoPCM5; (f) nanoPCM6; (g) nanoPCM7; (h) nanoPCM8

4. CONCLUSIONS

The stability of nanoPCMs is a major research challenge, as it will determine their potential application in practice. At present, there is no reliable method for assessing the stability of produced nanoPCMs. As stated by Saydam and Duan [25], multidisciplinary efforts to achieve a better understanding of the physical/chemical properties of nanoPCMs are required.

The paper presents the original results of stability studies of a series of fatty acid-based nanocomposites with the use of two types of nanoparticles and two stability-enhancing surfactants. Out of eight samples tested (as presented in Tab. 1), only two can be considered relatively stable, i.e. nanoPCM1 and nanoPCM7, and these are characterised by smaller nanoparticle concentrations. In the case of addition of Al_2O_3, it was observed that regardless of the concentration of nanoparticles (1%wt or 5%wt), nanoPCMs with OA surfactant were more stable. For nanoPCMs with TiO_2 nanoparticles, also irrespective of the nanoparticle concentration (1% wt or 5% wt), those in which PVP was used as a surfactant were more stable.

In addition to assessing the stability of nanoPCM, the effect of nanoparticles on the rate of heat transfer during the process of heating and cooling nanoPCM was assessed. It was observed that, regardless of surfactant type (OA or PVP), addition of Al_2O_3 nanoparticles results in heat transfer deterioration, particularly during the melting process. Contrary to the effect observed with Al_2O_3 nanoparticles, addition of TiO_2 nanoparticles, particularly when administered in the combination of OA surfactant, results in heat transfer enhancement, particularly during the melting process.

A thermal stability test of the produced nanocomposites, based on temperature measurement in the axis of the cylindrical sample placed in a constant temperature bath, was also proposed.

NOMENCLATURE

c_p	Specific heat	[J/(gK)]
T'_k	Initial solidification temperature	[K]
T''_k	Final solidification temperature	[K]
T'_t	Initial melting temperature	[K]
T''_t	Final melting temperature	[K]

ABBREVIATIONS

BM	BPCM melting
BPCM	Base phase change material
BS	BPCM solidification
DSC	Differential scanning calorimetry
EDS	Energy dispersive spectroscopy
FESEM	Field emission scanning electron microscopy
FT-IR	Fourier transform infrared spectroscopy
GNP	Graphene nanoplatelets
HSL	Hue-saturation-lightness
MWCNT	Multi-walled carbon nanotubes
OA	Oleic acid
PCM	Phase change material
PVP	Polyvinylpyrrolidone
RGB	Red-Green-Blue
SDBS	Sodium dodecyl benzene sulfonate
SEM	Scanning electron microscopy

REFERENCES

1. Haghighi EB, Nikkam N, Saleemi M, Behi M, Mirmohammadi MA, Poth H, et al. Shelf stability of nanofluids and its effect on thermal conductivity and viscosity. Measurement Science and Technology. 2013;24;105301.
2. Lotfizadeh Dehkordi B., Ghadimi A., Metselaar H.S.C. Box–Behnken experimental design for investigation of stability and thermal conductivity of TiO_2 nanofluids. Journal of Nanoparticle Research. 2013;15:1369.
3. Witharana S., Palabiyik I., Musina Z., Ding Y. Stability of glycol nanofluids — The theory and experiment. Powder Technology. 2013;239:72–77.
4. Ilyas S.U., Pendyala R., Marneni N. Stability and Agglomeration of Alumina Nanoparticles in Ethanol-Water Mixtures. Procedia Engineering. 2016;148:290–297.
5. Fuskele V., Sarviya R.M. Recent developments in Nanoparticles Synthesis. Preparation and Stability of Nanofluids. Materials Today: Proceedings. 2017;4:4049–4060.
6. Yu F, Chen Y, Liang X, Xu J, Lee C, Liang Q, et al. Dispersion stability of thermal nanofluids. Progress in Natural Science: Materials International. 2017;27:531-542.
7. Abdullah M, Malik SA, Iqbal MH, Sajid MM, Shad NA, Hussain SZ, et al. Sedimentation and stabilization of nano-fluids with dispersant. Colloids and Surfaces. 2018;554;86–92.
8. Mahbubul IM, Elcioglu EB, Amalina MA, Saidur R. Stability, thermophysical properties and performance assessment of alumina–water nanofluid with emphasis on ultrasonication and storage period. Powder Technology. 2019;345:668–675.

9. Lee L, Han K, Koo J. A novel method to evaluate dispersion stability of nanofluids. International Journal of Heat and Mass Transfer. 2014;70;421–429.
10. Lemes MA, Rabelo D, de Oliveira AE. A novel method to evaluate nanofluid stability using multivariate image analysis. Analytical Methods. 2017;9;5826.
11. Ilyas SU, Pendyala R, Marneni N. Stability of nanofluids. Topics in Mining, Metallurgy and Materials Engineering. Eds. Korada VS, Hamid NHB. Engineering applications of nanotechnology. From energy to drug delivery. Springer;2017. Avaiable from: https://www.springerprofessional.de/engineering-applications-of-nano technology/11992454
12. Wu S, Zhu D, Zhang X, Huang J. Preparation and Melting/Freezing Characteristics of Cu/Paraffin Nanofluid as Phase-Change Material (PCM). Energy Fuels. 2010; 24(3):1894–1898.
13. Choi DH, Lee J, Hong H, Kang Y T. Thermal conductivity and heat transfer performance enhancement of phase change materials (PCM) containing carbon additives for heat storage application. International Journal of Refrigeration. 2014;42:112-120.
14. Jin Y, Wan Q, Ding Y. PCMs Heat Transfer Performance Enhancement with Expanded Graphite and its Thermal Stability. Procedia Eng. 2015;102:1877-1884
15. Zhichao L, Qiang Z, Gaohui W. Preparation and enhanced heat capacity of nano-titania doped erythritol as phase change material. International Journal of Heat and Mass Transfer. 2015;80;653–659.
16. Nourani M, Hamdami N, Keramat J, Moheb A, Shahedi M. Thermal behavior of paraffin-nano-Al_2O_3 stabilized by sodium stearoyl lactylate as a stable phase change material with high thermal conductivity. Renewable Energy. 2016;88:474-482.
17. Liu Y, Yang Y. Use of nano-α-Al_2O_3 to improve binary eutectic hydrated salt as phase change material. Solar Energy Materials & Solar Cells. 2017;160;18–25.
18. Singh DK, Suresh S, Singh H, Rose BAJ, Tassou S, Anantharaman N. Myo-inositol based nano-PCM for solar thermal energy storage. Applied Thermal Engineering. 2017;110;564–572.
19. Zhang JL, Wu N, Wu XW, Chen Y, Zhao Y, Liang JF, et al. High latent heat stearic acid impregnated in expanded graphite. Thermochimica Acta. 2018;663;118–124.
20. Nourani M, Hamdami N, Keramat J. Preparation and evaluation of a stable nanoalumina-paraffin composite: Melting rate investigation using image analysis. Journal of Dispersion Science and Technology. 2018;39(10);1385-1393.
21. Prabhu B, ValanArasu A. Stability analysis of TiO_2–Ag nanocomposite particles dispersed paraffin wax as energy storage material for solar thermal systems. Renewable Energy. 2020;152;358-367.
22. Ibrahim SI, Ali AA., Hafidh SA, Chaichan MT, Kazem HA, Ali JM, Isahak WNR, Alamiery A. Stability and thermal conductivity of different nano-composite material prepared for thermal energy storage applications. South African Journal of Chemical Engineering. 2022;39;72-89.
23. Zhang G, Guo Y, Zhang B, Yan X, Lu W, Cui G, Du Y. Preparation and control mechanism of nano-phase change emulsion with high thermal conductivity and low supercooling for thermal energy storage. Energy Reports. 2022;8;8301-8311.
24. Venkateshwar K, Joshy N, Simha H, Mahmud S. Quantifying the nanoparticles concentration in nano-PCM. Journal of Nanoparticle Research. 2019;21;260.
25. Saydam V, Duan X. Dispersing Different Nanoparticles in Paraffin Wax as Enhanced Phase Change Materials – A Study on the Stability Issue. Journal of Thermal Analysis and Calorimetry. 2018;135(1):
26. Lee W, Yeop J, Heo J, Yoon YJ, Park SY, Jeong J, et al. High colloidal stability ZnO nanoparticles independent on solvent polarity and their application in polymer solar cells. Scientific Reports. 2020;10:18055.
27. Rajendran D, Ramalingame R, Adiraju A, Nouri H, Kanoun O. Role of Solvent Polarity on Dispersion Quality and Stability of Functionalized Carbon Nanotubes. Journal of Composites Science. 2022;6(1):26
28. Saroha J, Mehra S, Kumar M, Sharma SN. Thermo-physical properties of paraffin/TiO_2 and sorbitol/TiO_2 nanocomposites for enhanced phase change materials: a study on the stability issue. Applied Physics A. 2021;127:916.

Janusz T. Cieśliński https://orcid.org/0000-0002-8919-984X
Paulina Boroń https://orcid.org/0009-0006-0263-3997
Maciej Fabrykiewicz https://orcid.org/0000-0001-7648-8629